

# Enhanced Mixing of Supersonic Jets

T. G. Tillman,\* W. P. Patrick,† and R. W. Paterson‡

United Technologies Research Center, East Hartford, Connecticut 06108

An experimental study of supersonic mixer nozzles in a coflowing stream has been conducted in the United Technologies Research Center open jet acoustic wind tunnel. Enhanced supersonic jet mixing is important in a number of applications including jet exhaust noise reduction and improved flow distribution within engine combustors. Recently discovered novel concepts promoting enhanced mixing via the introduction of axial vorticity into the exhaust have resulted in studies of the mixing process for nozzles operating at low, subsonic Mach number conditions and low temperatures. The goal of the present experimental study was to evaluate these approaches to jet mixing in the high-temperature, supersonic primary flow regime typical of turbofan/turbojet engine operation. Jet total temperature, total pressure, static pressure, and velocity distributions were measured to characterize the mixing process for baseline slot and circular nozzles, and for several mixer nozzles. The measurements were made at a jet exit Mach number of 1.5, a wind-tunnel forward flight Mach number of 0.5, and a jet total temperature of 1000°F. A principal conclusion of this study is that the axial vorticity mixing mechanism previously shown to be responsible for rapid mixing in low-speed, subsonic flows is also effective in a supersonic flow environment. Reductions in nozzle potential core length of approximately a factor of two relative to the slot nozzle configuration were observed for one of the mixer nozzles studied.

## Nomenclature

$A$	= area, in. <sup>2</sup>
$A^*$	= nozzle throat area, in. <sup>2</sup>
$AR$	= aspect ratio
$b$	= two-dimensional nozzle width (long dimension, in.)
$d_{eq}$	= diameter of equivalent area circular nozzle, in.
$d_j$	= circular nozzle exit diameter, in.
$h$	= nozzle exit height (short dimension, in.)
$M_o$	= tunnel freestream Mach number
$M_j$	= nozzle exit Mach number
$N_T$	= jet centerline total temperature decay exponent
$N_u$	= jet centerline velocity decay exponent
$P_T$	= total pressure, psia
$P_{T_o}$	= tunnel freestream total pressure, psia
$P_{T_p}, P_{T_j}$	= nozzle primary supply total pressure, psia
$Pr$	= Prandtl number
$R$	= radial distance, in.
$T_o, T_{T_o}$	= tunnel freestream total temperature, °F
$T_T$	= total temperature, °F
$T_{T_p}, T_{T_j}$	= nozzle primary supply total temperature, °F
$U$	= velocity, ft/s
$x$	= axial coordinate, in.
$y$	= transverse coordinate, in.
$z$	= vertical coordinate, in.

## Introduction

THE overall issue addressed in this article is the enhancement of mixing rates in supersonic jet flows by the use of mixer nozzles. The present study examines supersonic jet mixing rates in an unconfined, coflowing secondary airstream. Enhanced supersonic jet mixing is important in a number of applications including jet exhaust noise reduction and im-

proved flow distribution within engine combustors. Nozzle shapes similar to the types considered here are used in turbofan engines such as the P&W JT8D to mix subsonic fan and core engine streams prior to discharge and thereby reduce jet exhaust noise. In addition, there has been recent interest in the use of these nozzles to more thoroughly mix primary and secondary flows in ejectors, which results in increased ejector performance.

Jet mixing has been the subject of a variety of experimental and analytical work which has been done over the years. The historical progression of research in this area begins with circular jets, and proceeds through rectangular jets and forced mixers. A detailed review of conventional jet mixing for circular and rectangular nozzles is provided by Tillman et al.<sup>1</sup>

The circular-nozzle jet mixing process is well understood<sup>2,3</sup> and is dominated by momentum transfer through the action of viscous shear stresses and small-scale turbulence in the mixing layer. Some of the first attempts to enhance the jet mixing process involved the use of rectangular nozzles. Here, jet mixing is still dependent on viscous shear stresses and small-scale turbulence transport. Mixing improvements relative to axisymmetric nozzles of the same exit area are the result of the distribution of shear stresses over a larger surface area.<sup>4-8</sup> Although rectangular nozzles have proven successful in increasing jet

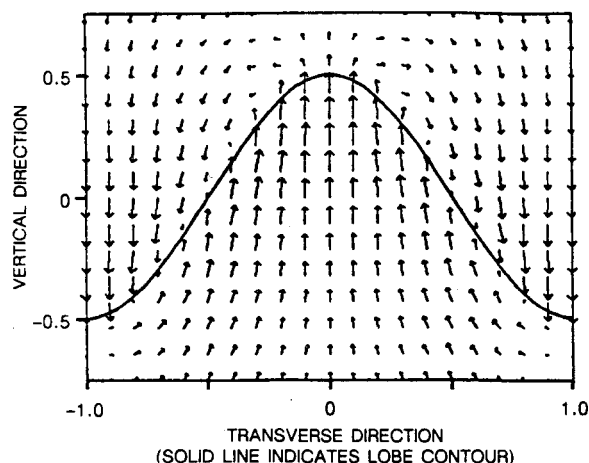


Fig. 1 Low-speed mixer lobe secondary velocity field measured by LDV.<sup>17</sup>

Presented as Paper 88-3002 at the AIAA/SAE/ASME/ASME 24th Joint Propulsion Conference, Boston, MA, July 11-13, 1988; received Aug. 7, 1989; revision received April 27, 1990; accepted for publication April 30, 1990. Copyright © 1991 by the United Technologies Corporation. Published by the American Institute of Aeronautics and Astronautics, Inc., with permission.

\*Research Engineer, Mail Stop 17, Silver Lane. Member AIAA.

†Senior Project Engineer. Member AIAA.

‡Manager, Aerodynamics and Environmental Sciences. Associate Fellow AIAA.

mixing rates, size and weight requirements place practical upper limits on nozzle aspect ratio, and hence mixing effectiveness, for many exhaust system installations. Forced mixer nozzles attempt to enhance the natural mixing process by introducing additional mechanisms.

One of the first comprehensive analytical and experimental studies of mixer nozzle flows was reported by Paynter et al.<sup>9</sup> in 1977. In this study, lobed mixers were used as a means to enhance mixing for jet noise reduction. Some early work was also done by Bevilacqua,<sup>10,11</sup> and Dejoode and Patankar,<sup>12</sup> on hypermixing for thrust augmenting ejectors and nozzles. In the hypermixing concept, an array of alternately canted nozzles was used to generate intense, small streamwise vortices at the adjacent nozzle interfaces. The streamwise vortices aided in the mixing process by entraining additional external (secondary) fluid into the mixing region, and by increasing the natural turbulence spreading process within this region. Associated with the production and mixing-out of these intense vortices, however, were large losses that can limit thrust augmentation benefits.

Building on the results of early forced mixer nozzle work, Paterson<sup>13</sup> performed an experimental study of a turbofan mixer nozzle flowfield in which laser Doppler velocimetry (LDV) measurements revealed strong radial velocities at the exit plane of the nozzle. These radial velocities, flowing in opposite directions in the secondary and primary lobes, generated large-scale, low-intensity axial vortices with a characteristic dimension on the order of the lobe height. A principal conclusion of Paterson's study was that the large-scale secondary flows present in the flowfield of this type of forced mixer control the mixing process by sweeping large amounts of secondary flow into the primary core. In addition, it was found that by producing large-scale, low-intensity vortices without flow separation within the nozzle, high downstream mixing rates could be achieved while not incurring significant total pressure losses.

Subsequent to this experiment, a series of low-speed, low-temperature studies were performed to examine the axial vorticity mixing process more thoroughly. Tillman et al.<sup>1</sup> discuss the highlights of these efforts in detail. Advances in forced mixer lobe designs are presented by Presz et al.<sup>14,15</sup> in two papers describing the use of forced mixer lobes in ejectors. Lobe design was found to be critical to good forced mixer performance. Werle et al.<sup>16</sup> investigated the details of the flow structure in an axial vortex array generated by forced mixer lobes. Experiments, analytical work predicting the large-scale, secondary flows, and water tunnel flow-visualization studies which showed the vortex roll-up process occurring downstream of the lobe trailing edge were performed. Skebe et al.<sup>17</sup> examined both analytically and experimentally the near-lobe flowfield for several advanced forced mixer lobes, documenting the vortex formation process and the sensitivity of the lobe design to mixing performance. Figure 1 shows LDV measurements of the secondary velocity field just downstream of a forced mixer lobe taken from Skebe's<sup>17</sup> experiment. A pair of

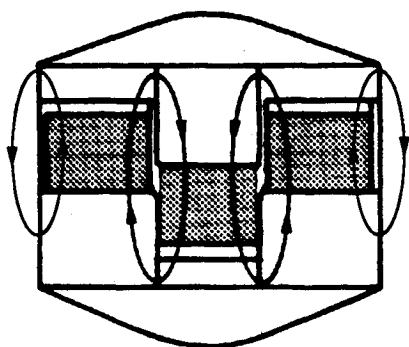


Fig. 2 Splayed nozzle forced mixer lobes (end view).

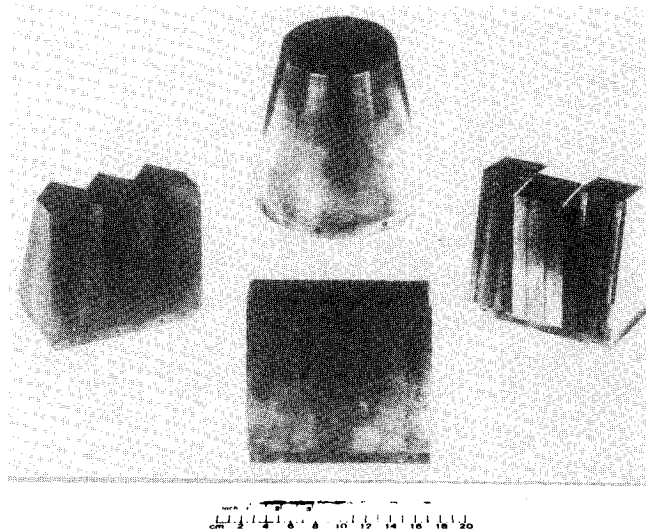


Fig. 3 Supersonic nozzle models.

counter-rotating, large-scale streamwise vortices is clearly seen.

In addition to the use of forced mixer nozzles, there have been other attempts to enhance jet mixing. Gutmark and Schadow<sup>18</sup> and Husain and Hussain<sup>19</sup> have studied elliptic nozzles and found that they can provide a mixing benefit relative to conventional round nozzles. Acoustic feedback and the presence of normal shock waves in the flowfield have also been shown to be capable of providing mechanisms for mixing enhancement.<sup>8,20,21</sup> Furthermore, the use of forced unsteadiness in mixing layers has been explored as a method by which to enhance jet mixing.<sup>22-24</sup> In this case the term "forced" refers to active periodic forcing of the shear layer, as opposed to the passive vectoring of one flowstream into another in the case of forced mixer nozzles.

The goal of the present study was to establish whether the streamwise vorticity mixing mechanism, which is known to be responsible for rapid, subsonic mixing within turbofan forced mixer nozzles and mixer ejectors, also provides enhanced jet mixing for an unconfined supersonic jet issuing into a coflowing subsonic stream. The two main differences, therefore, between established mixing technology and the focus of the present work are 1) mixing between a supersonic jet and a subsonic coflowing stream, and 2) the absence, in this case, of a confining mixing duct (i.e., external rather than internal mixing).

The present approach was to conduct supersonic nozzle jet mixing tests at elevated temperature within a coflowing wind-tunnel airstream. Measurements of total temperature, total pressure, static pressure, and velocity were performed within the jet to characterize the mixing process. Jet mixing was defined for conventionally shaped baseline nozzles, and for several mixer nozzles. Figure 2 shows an example of mixer lobe geometry for one of the supersonic mixer nozzles tested during the present study. The axial vortex pattern that is established by the mixer lobes is indicated.

A principal result from this experimental study is that the axial vortex mechanism previously shown to be responsible for rapid mixing in low-speed, subsonic flows is also effective in the supersonic flow regime. A reduction in potential core length of approximately a factor of two relative to a baseline rectangular nozzle was observed for one of the mixer nozzles. A second result was that a set of data on jet development was obtained for use in assessing computational fluid dynamics (CFD) procedures for calculating complex nozzle exhaust flowfields. Finally, laser Doppler velocimetry (LDV) techniques yielding reliable high-temperature, supersonic jet three-dimensional velocity data were developed and exercised. Comparisons with axial velocity data derived from jet total pressure and static pressure measurements were favorable.

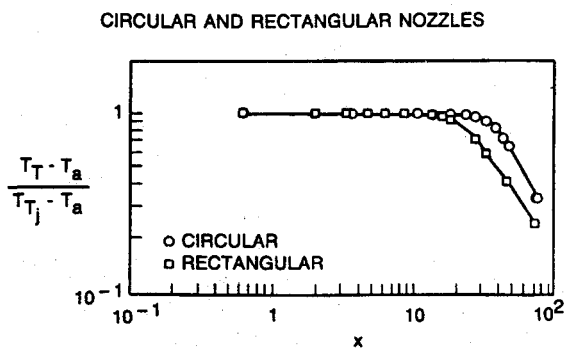


Fig. 4 Comparison of total-temperature potential core length.

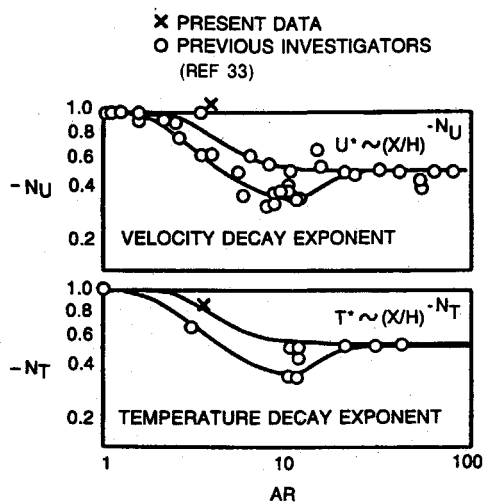


Fig. 5 Two-dimensional jet near-field decay exponents from previous investigations.

### Description of Experiment

The present study was performed in the United Technologies Research Center (UTRC) open jet acoustic wind tunnel. This tunnel was built in 1969 for aircraft propulsion system noise research. The low freestream turbulence levels have made airfoil boundary-layer work possible, and the open jet test section arrangement is particularly well suited for the study of jet aerodynamics. A paper describing the design of the tunnel is given by Paterson et al.<sup>25</sup>

A 400-psi high-pressure air system is used to provide airflow to the supersonic nozzle propulsion models tested in this facility. A propane heater located at the acoustic tunnel is capable of heating the air to a maximum temperature of 1000°F to simulate the hot jet exhaust. A total of seven supersonic nozzle models were designed and fabricated for this experiment. Three were axisymmetric designs, and four were designed as two-dimensional nozzles. The two-dimensional baseline rectangular nozzle exit dimensions were 5.78 × 1.57 in. ( $AR = 3.7$ ), and the circular nozzle exit diameter was 3.42 in. The splayed mixer nozzle was designed with three equal-area,  $AR \cong 1$  primary lobes. The lobes were inclined relative to the wind-tunnel streamwise direction at an angle of +18 deg on the top surface and -6 deg on the bottom surface, yielding an average inclination angle of +6 deg for the entire lobe. All of the models were capable of operating with 1000°F heated primary flow, and each model was specifically designed for the same value of  $A_{exit}/A^*$ . This value was selected such that the nozzle exit Mach number was 1.5. In addition to sizing the models for the same values of  $A_{exit}/A^*$ , care was taken to insure that each model had the same exit area. Thus, the mixer nozzles were different from the baseline models (i.e., circular and rectangular nozzles) only in exit shape—areas, area ratios,

and in the case of the two-dimensional models the nozzle width  $b$ , were all the same for each nozzle. This area symmetry among the various models is important, because with it the nozzles operate at nominally the same design condition, and a meaningful comparison of mixing effectiveness between the lobed nozzles and the baseline nozzles can be made.

Figure 3 shows a photograph of the four nozzles discussed in this article. It should be noted that the splayed mixer nozzle, while generically similar to the hypermixing concept of Bevilacqua,<sup>10,11</sup> generates large-scale, low-intensity vortices without flow separation within the nozzle. This allows for high downstream mixing rates to be achieved without incurring significant total pressure losses.

Detailed jet mapping of total temperature, total pressure, and static pressure was accomplished by the use of a combination probe attached to a remotely actuated, computer-controlled traverse system. This probe is described by Tillman et al.<sup>1</sup> The total temperature portion is a 1/4-in.-diam, double-radiation-shielded probe consisting of a chromel-alumel thermocouple surrounded by two concentric radiation heat loss shields. Radiation losses from unshielded thermocouples in these types of applications (i.e., a spatially small, hot jet surrounded by a cold ambient with a large temperature gradient separating the two) dictate the need for radiation shielding. Radiation-shielded total-temperature probes have been developed extensively by Moffat.<sup>26,27</sup>

Jet total pressure was measured for some of the nozzles using a standard impact-type pitot tube. Static pressure measurements were then used to correct the measured total pressure for normal shock losses encountered when a pitot tube is placed in a supersonic flow. A specially designed shielded supersonic total pressure probe was used in the near-field of the mixer nozzles, where velocity inflow angles relative to the probe could be large. This probe was an adaptation of an aspirated Kielhead total pressure probe used previously in subsonic flow by Patrick.<sup>28</sup> Calibration up to Mach numbers of 1.6 confirmed that the probe recovered vector total pressure (downstream of any probe-induced shock losses) to within 1.5% for velocity inflow angles up to 35 deg. Measurement accuracy for this probe increases with decreasing inflow angle and Mach number. Maximum flow angles near the exit plane of the mixer nozzles were estimated to be in the 15–20 deg range, based on nozzle geometry. Jet static pressure was measured with a specially designed supersonic static pressure probe. This probe was developed by Pinckney,<sup>29</sup> and was used by Simonich et al.<sup>30</sup> The probe is designed to recover the stream static pressure a small number of diameters downstream of the probe leading edge. An array of four commonly manifolded static pressure holes equally spaced circumferentially around the probe azimuth is used in this design. Pinckney calibrated this probe at a Mach number of 2.5 and found it to read accurately (to within approximately  $\pm 0.25\%$ ) up to velocity inflow angles of 8 deg.

The laser velocimetry (LV) system employed in this experiment was a TSI 9100-7, four-beam, two-color system that measured two mutually perpendicular velocity components simultaneously. The system used a 4-W argon-ion laser with a color splitter and beam splitters to divide the optical power equally between blue (488.0 nm) and green (514.5 nm) beams. The beams were inclined to the main stream direction at a 45-deg angle to permit the measurement of both the streamwise and transverse components of velocity without Bragg-shifting the transmitted beams. The Doppler-shifted scattered light was collected in the backscatter mode and analyzed with a counter-type signal processor having a 200-MHz Doppler frequency capability.

Seeding of both the primary and secondary streams was accomplished with 1- $\mu$ m-diam  $TiO_2$  particles using multiple independently controlled fluidized bed seeders. One high-pressure seeder was used to inject  $TiO_2$  particles into the primary supply piping upstream of the propane heater. Four lower-pressure seeders, manifolded to provide separate con-

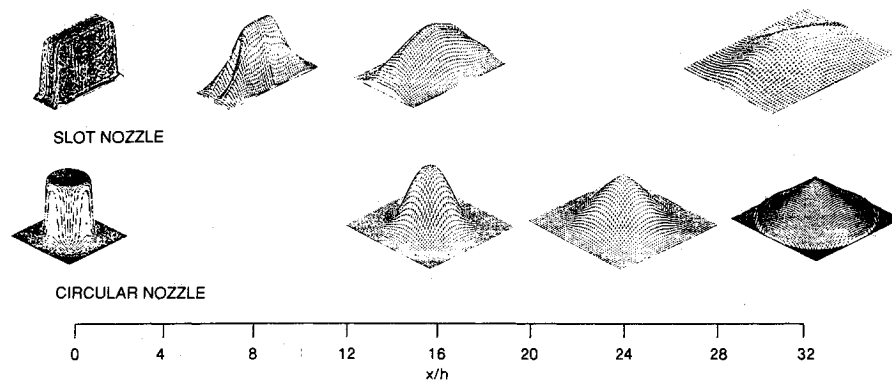


Fig. 6 Total-temperature profiles for supersonic exhaust jets.

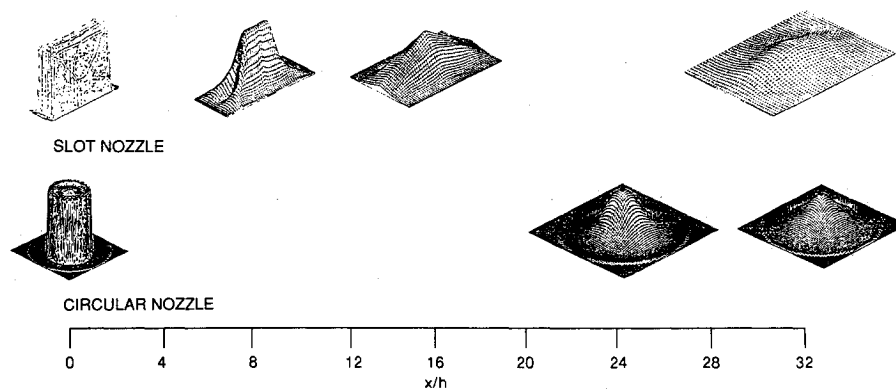


Fig. 7 Total-pressure profiles for supersonic exhaust jets.

trol over the seed density in two radial zones of the coflowing stream, supplied seed through eight radially and azimuthally spaced seed-injection tubes located downstream of the turbulence control screens in the acoustic tunnel inlet.

To measure three velocity components with the two-component system, two separate test runs were made at each measurement plane. Between tests, the nozzle was rotated 90 deg to enable the LV system to measure a third orthogonal component relative to the coordinate system fixed in the nozzle exit plane.

Nozzle and tunnel operating conditions were selected such that an adequate simulation of a generic exhaust system was achieved. Measurements were made at a jet exit Mach number of 1.5, a wind-tunnel forward flight Mach number of 0.5, and an exhaust total temperature of 1000°F. The primary objective of this experiment was to evaluate the axial vorticity mixing concept relative to high-temperature, supersonic nozzle operation. It has been shown in a recent study by Greitzer et al.<sup>31</sup> that a substitution principle exists for nonisentropic, viscous, heat-conducting flows. This principle states that Mach number and total pressure distributions in these types of flows are independent of temperature over a wide range. Practically, this means that useful mixing results, applicable to a range of nozzle flow stagnation temperatures, may be obtained by performing an experiment at a single primary-flow stagnation temperature.

## Results and Discussion

### Baseline Nozzles

The experiments conducted in the present study have resulted in nozzle centerline decay documentation and detailed jet flowfield mapping for both the circular and rectangular baseline nozzles. This process was accomplished so that 1) conventional mixing in the high-temperature, supersonic flow regime could be studied relative to the work of previous in-

vestigators, who have focused primarily on low-speed jets in the absence of forward flight, and 2) a set of detailed data would exist to aid in the CFD code development process for the calculation of complex jet flowfields. In addition, these nozzles provide a baseline set of data that may be used to evaluate the effectiveness of the mixer nozzles. The present study has also aimed to demonstrate the viability of three-dimensional LDV techniques to quantify jet velocities for supersonic, high-temperature nozzle operating conditions. This is an important diagnostic tool that may be used in the future to characterize the secondary flows responsible for enhanced mixing in the mixer nozzle flowfields.

The centerline total temperature decay characteristics for the two nozzles are shown in Fig. 4. The effect of aspect ratio on the potential core length is clearly seen, with the core of the rectangular nozzle ( $AR = 3.7$ ) shorter than that of the circular nozzle ( $AR = 1$ ) by approximately a factor of two. A similar centerline decay trend was observed in the total pressure data for the two nozzles, although slightly more scatter was present. This scatter was a result of the presence of shock waves in the jet, which made pressure measurement more difficult and subject to error. Under this condition, the measurement of static pressure is difficult, and since this measurement was used to correct the total pressure for pitot probe shock losses, it is not surprising that some data scatter is present in the final shock-corrected values. The nozzle near-field exhaust was examined using a shadowgraph system, and shock-wave patterns were observed downstream of the nozzle exit. These shocks resulted primarily from the internal nozzle design that lacked shock-free contoured surfaces in the supersonic section, thus providing an inability to achieve a perfectly expanded operating condition. The presence of shock patterns in rectangular supersonic jets has been previously noted by Putnam and Mercer<sup>32</sup>; similar observations were made in the present experiment relative to both the rectangular and circular nozzles. Some of the total-pressure data will be shown in subsequent figures.

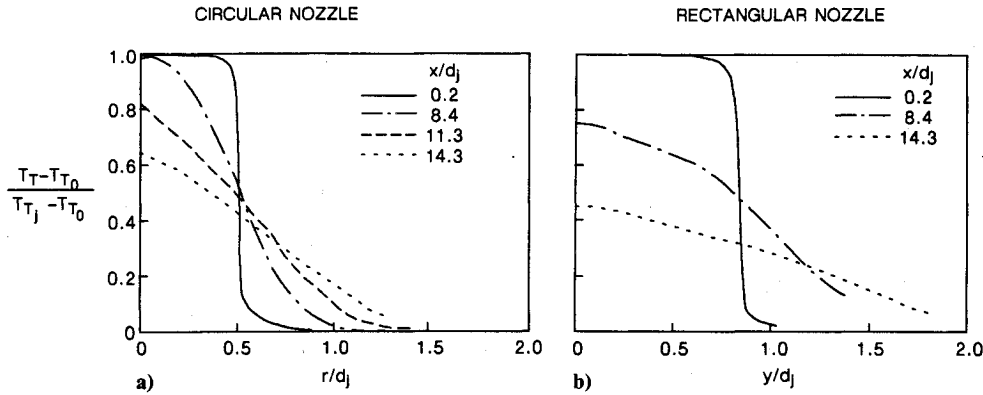


Fig. 8 Baseline nozzle radial total-temperature profiles.

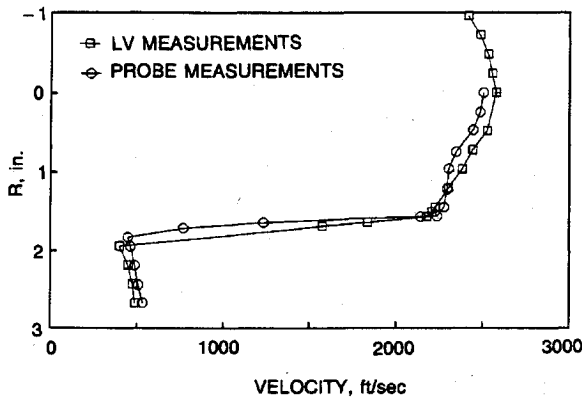


Fig. 9 Baseline circular nozzle velocity measurements at  $x/d_j = 0.2$ , LV vs probe measurements.

Figure 5 shows the velocity and temperature decay exponents (for the near-field decay region of the rectangular nozzle flowfield) obtained from the present experiment relative to those obtained by others.<sup>33</sup> The two lines that are drawn on each of the plots shown in this figure bracket the scatter of the data obtained by previous investigators. The present values are seen to be reasonable.

Jet flowfield mapping data were obtained in the form of transverse ( $y$ - $z$ ) profiles of total temperature and total pressure at several fixed axial locations for each of the two baseline nozzles. Figure 6 shows the total temperature data, and Fig. 7 the total pressure data. Four axial planes of data were obtained for each nozzle: one at the nozzle exit plane, one near the end of the potential core, and two in the downstream mixing region. For the rectangular nozzle, surveys consisting of several hundred points were performed over one quadrant of the nozzle flowfield. The data were then symmetrically projected into the other quadrants to create the surface

patterns shown in the figures. For the round nozzle, a single densely spaced radial survey was taken and the data were projected circumferentially to create the surface patterns. Each pair of intersecting lines on each of the surfaces corresponds to a data point. There was no smoothing or interpolation of these data.

Several features of the jet profiles are of interest. At the nozzle exit plane, it is noted that an uneven total pressure distribution exists for both nozzles, with local regions of low total pressure. This feature is attributed to the presence of shock waves, as mentioned earlier. In addition, the rectangular nozzle is seen to display better mixing and larger spreading rates locally in the corner regions. This effect is due to the presence of corner vortices developed in the circular-to-rectangular transition regions of the nozzle, and has been previously observed by others.<sup>32</sup> The same mixing features for the two nozzles which were noted in the centerline data are apparent in the detailed flowfield data. That is, the rectangular nozzle mixing rate is larger than that for the circular nozzle, due to the distribution of viscous shear stresses over a larger nozzle surface area. In addition, the thermal spreading of each jet is seen to be larger than the corresponding spreading of momentum (see Figs. 6 and 7). This is a feature that has been well documented by others,<sup>2,34</sup> and that one would expect in flows where  $Pr < 1$ . Figure 8 shows an alternate comparison of the two nozzles in the form of radial profiles of total temperature.

In short, the mixing process for the circular and rectangular nozzles exhibits the classic features observed previously by other investigators for jets operating across a wide spectrum of conditions. Similarity to previous work is displayed in such areas as the effect of nozzle aspect ratio, rectangular jet spreading characteristics, and jet centerline decay rates. The (conventional) mixing process is dominated by viscous shear-layer spreading, and by small-scale turbulence in the mixing region. Operating these conventional nozzles in a high-temperature, supersonic-flow environment in the presence of forward flight does not appear to appreciably alter the mixing

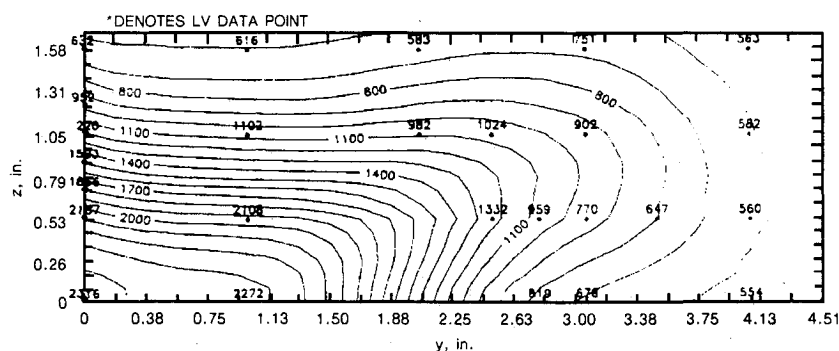


Fig. 10 Baseline rectangular nozzle velocity measurements at  $x/h = 8.4$ , LV vs probe measurements (velocities in ft/s).

process relative to behavior observed by others at low-temperature and subsonic operating conditions.

In addition to examining the mixing process for the baseline nozzles, the present experiment demonstrated the capability to successfully apply three-dimensional LDV techniques to the measurement of high-temperature supersonic jet velocities. Since the exhaust total temperature was 1000°F, supersonic velocities in excess of 2000 ft/s were present in the flowfield. As described earlier, a two-component LDV system was used to measure three components of mean velocity in the jet exhaust. Figures 9 and 10 show comparisons of LDV acquired axial velocity data with that derived from probe measurements of total pressure and static pressure, for both the circular and rectangular nozzles. Figure 9 shows excellent agreement between the two sets of measurements for a radial survey performed just downstream of the circular nozzle exit plane. Figure 10 shows LDV data points as they fall on a contour plot of the probe-measured axial velocity data at the location  $x/h = 8.4$  for the rectangular nozzle. Except for a few selected points, agreement is generally within several percent. These encouraging results indicate that LDV techniques may be useful in future experiments to document the secondary flows responsible for enhanced mixing in the high-temperature, supersonic jet exhaust of mixer nozzles.

#### Mixer Nozzles

Now that the mixing process for the baseline nozzles is understood, the additional benefits of the mixer nozzles may be examined. As previously described, the intent of these nozzles is to generate large-scale axial vorticity that will sweep large amounts of secondary fluid into the jet core and thereby accelerate the mixing process. Several mixer nozzles were studied experimentally, and results for two configurations are shown in Fig. 11.

In this figure, nondimensional centerline total temperature decay is plotted as a function of  $x/h$ , where  $h$  is the narrow exit dimension of the rectangular nozzle. Two mixer nozzles (sawtooth and splayed) are shown together with the baseline rectangular nozzle; these models are pictured in Fig. 3. One immediately notices the large reduction in potential core length for the splayed nozzle relative to the baseline rectangular nozzle. The length is reduced from  $x/h \approx 12$  to  $x/h \approx 6$ .

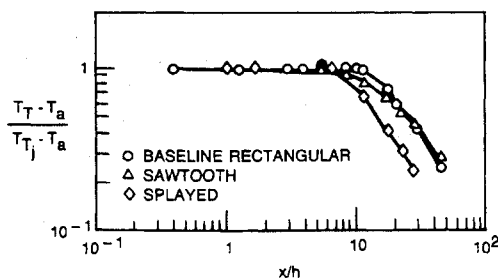


Fig. 11 Jet centerline total-temperature decay for two-dimensional nozzles.

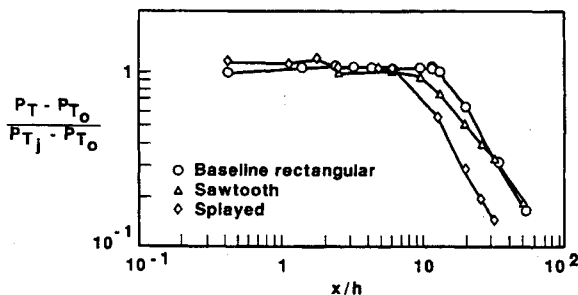


Fig. 12 Jet centerline total-pressure decay for two-dimensional nozzles.

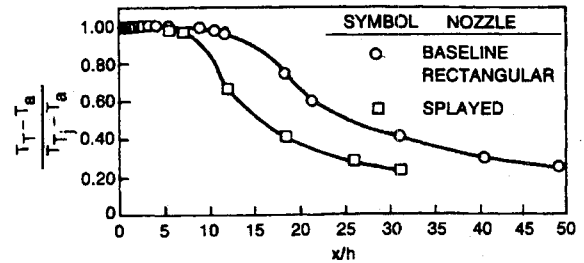


Fig. 13 Splayed nozzle mixing effectiveness.

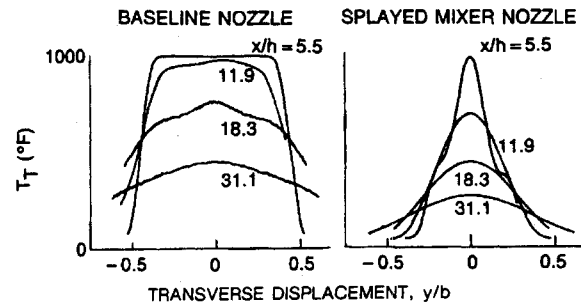


Fig. 14 Two-dimensional nozzle transverse total-temperature profiles.

This represents a significant improvement in mixing rate; at  $x/h = 12$ , the nondimensional total temperature for the rectangular nozzle is approximately 0.98, while the corresponding value for the splayed nozzle is approximately 0.65. At each downstream location in the flowfield, the jet centerline for the splayed nozzle was chosen to be the aerodynamic center of the middle lobe (see Fig. 1). The total-temperature and total-pressure levels in this portion of the jet were representative of the maximum levels encountered at any transverse or vertical location for each of the axial stations.

The sawtooth nozzle is seen to display only small mixing improvements relative to the baseline nozzle. Since the time of the design of these nozzles, analysis at UTRC<sup>16</sup> has shown that the splayed nozzle lobe design is more effective in generating large-scale, circulation-producing axial vortices than the lobes present on the sawtooth nozzle. It is for this reason that the sawtooth nozzle fails to meet the mixing performance of the splayed model. The same mixing characteristics are evident in Fig. 12, which shows the jet centerline nondimensional total-pressure decay for these three nozzles. It should be noted in Figs. 11 and 12 that the reduction in potential core length for the splayed nozzle relative to the baseline rectangular nozzle is accomplished without a downstream penalty in jet centerline decay rate. Figure 13, a linear-scale plot of nondimensional centerline total temperature for the rectangular and splayed nozzles, highlights the substantial mixing benefits of the splayed nozzle.

Although detailed mapping was not done for the splayed nozzle, transverse total-temperature profiles were obtained to highlight some of the key features of the mixing process. Figure 14 shows transverse profiles taken across the center of the long dimension ( $b$ ) of the baseline rectangular and splayed nozzles (again, for the splayed nozzle the profile was taken spanwise across the aerodynamic center of the middle lobe). These profiles are analog traces of the output from the total-temperature probe thermocouple as the probe was traversed slowly across the jet. The mixing benefits of the splayed nozzle are clear.

The profiles are flat and show maximum total temperatures near 1000°F for the rectangular nozzle at  $x/h$  values up to 11.9. At larger values of  $x/h$ , a shear-driven viscous decay reduces the jet total temperature and is responsible for the profile shape. The total-temperature distribution for the splayed nozzle is seen to be substantially different. At  $x/h =$

5.5, the decay process has already begun. By  $x/h = 11.9$ , the maximum temperature of the jet has dropped below 700°F, indicating a significantly different mixing process relative to that of the baseline nozzle. We feel that this enhanced mixing is attributed to the presence of axial vortices in the jet flowfield of the splayed nozzle. It is seen that mixing continues down to  $x/h = 18.3$ , where the change in peak temperature level from the previous axial station begins to approach that of the baseline nozzle, and the profile shapes begin to look similar between the two nozzles. By the time  $x/h = 31.1$  is reached, a fully developed profile shape exists.

We believe that the splayed nozzle mixing benefit relative to the rectangular nozzle seen in Figs. 11–14 is the result of an additional mechanism beyond conventional viscous spreading. It is believed that large-scale axial vortices are introduced into the flowfield due to the nozzle geometry, and that these vortices are responsible for bringing increased amounts of secondary and primary fluid into contact. Although the actual mixing process in both cases is due to the action of viscous forces and small-scale turbulence, we believe that the enhanced mixing benefit of the splayed nozzle is the result of an increased distribution of these quantities within the jet core due to the action of the vortices.

Evidence for this is shown in Fig. 15, which is a comparison of the measured and calculated splayed nozzle flowfields. The calculations were taken from Anderson and Barber.<sup>35</sup> The first part of the figure shows the calculated vs measured nozzle centerline axial total-temperature decay, where the aerodynamic centerline of the middle lobe was followed downstream as described above. The calculation is seen to match the experimental data reasonably well. The second part of the figure shows the nozzle exit plane secondary velocity field that was used in the calculation. The largest vectors in this figure correspond to secondary velocity magnitudes of approximately 15% of the nozzle exit (axial) velocity. Large-scale vortices are clearly present in the flowfield, and it was found that removing this vorticity from the calculation resulted in a significant reduction in mixing performance and a failure to match the experimental data.

Further evidence of enhanced mixing for the splayed nozzle is shown in Fig. 16. This figure shows a plot of the centerline total-temperature decay of the circular nozzle and that of the middle lobe ( $AR \approx 1$ ) of the splayed nozzle (treated as an isolated nozzle) as functions of  $x/d_{eq}$ . Previous investigators<sup>5,7</sup> have shown that for equal-aspect-ratio nozzles operating at the same condition, plotting the centerline axial decay characteristics as a function of  $x/d_{eq}$  will cause the data to collapse onto a single curve. Here  $d_{eq}$  is the diameter of a circular nozzle with an area equivalent to that of the nozzle in question.

Thus,  $d_{eq}$  for the circular nozzle is simply the nozzle exit diameter  $d_j$ , and the corresponding value for the splayed nozzle isolated lobe is the diameter of a circular nozzle that has the same area as the individual square lobe. The collapse of data when plotted in this manner has been verified experimentally for the specific case of round vs square  $AR = 1$  nozzles.<sup>7</sup> Thus, if the lobes of the splayed nozzle were simply behaving as individual conventional square nozzles, the data would match that of the circular nozzle.

Examination of Fig. 16 shows that the two present sets of data do not collapse onto a single curve. To the contrary, the potential core associated with the center lobe of the splayed nozzle is much shorter (by nearly a factor of two) than would be predicted by the nondimensional circular nozzle data. This indicates that the splayed nozzle exhaust is responding to something beyond the conventional jet mixing process.

At this point, it is important to remember how the nozzle areas were scaled. All of the nozzles were designed to have the same exit area, and the same value of  $A_{exit}/A^*$ . Thus, they all operated at nominally the same exit condition for a given nozzle pressure ratio setting. The changes in nozzle exit geometry between the mixer nozzles and the baseline nozzles resulted in only a change in exit shape. In the case of the two-dimensional mixer nozzles, the nozzle width  $b$  was also preserved relative to the baseline rectangular nozzle. Thus, all of the two-dimensional nozzles possessed the same effective height  $h$ . The result of this is that a true comparison may be made between the various nozzles to study mixing effectiveness. In addition, the baseline rectangular nozzle height is a reasonable parameter on which to nondimensionalize axial distances.

There are several other factors that influence the jet mixing process; these will be reviewed briefly. The presence of a co-flowing stream has been shown to have a pronounced effect on increasing jet potential core length. This has been documented by several investigators, including Schetz<sup>36</sup> and Weinstein et al.<sup>37</sup> In addition to this phenomenon, jet exit Mach number also affects the potential core length. Increasing the exit Mach number tends to increase the potential core length; experiments by Lau<sup>2</sup> and by Simonich et al.<sup>30</sup> have documented this effect. Another element that should be considered is the potential core length response to jet heating. Lau<sup>2,3</sup> found that heating the primary flow causes the jet potential core length to contract. The contraction continues up to a limiting temperature ratio of 1.5, beyond which the length remains unchanged. Lau further found that heating the jet does not alter the shear-layer spreading rate, a finding consistent with that of Greitzer et al.<sup>31</sup>; the reduction in potential core length is accomplished by a rotation of the entire shear layer toward the jet axis. Finally, the presence of shock waves and acoustic feedback in

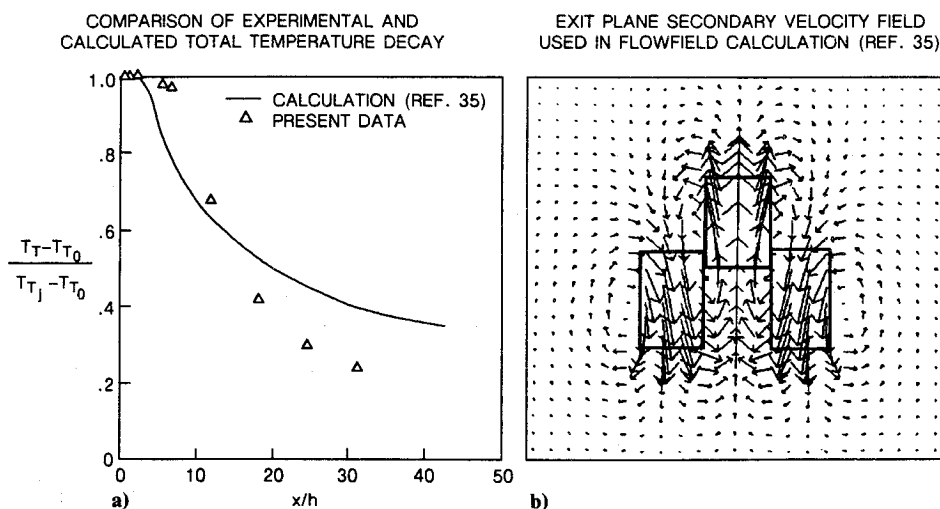


Fig. 15 Splayed nozzle flowfield calculation results.



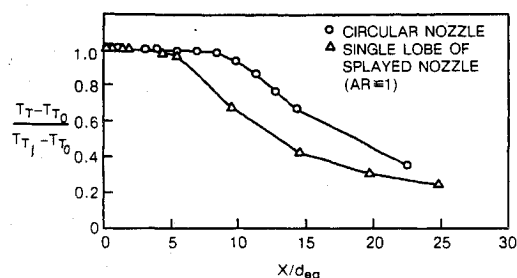


Fig. 16 Mixing of splayed nozzle  $AR \approx 1$  lobe vs circular nozzle.

the jet flowfield has been shown to be capable of significantly affecting the mixing process<sup>8,20,21</sup> in supersonic flows.

The above effects are described so that the appropriate care may be taken in evaluating nozzle mixing effectiveness when comparing the work of different investigators. The present experiment examines high-temperature, supersonic jets in the presence of a compressible, subsonic coflowing stream, and many of the effects mentioned above are present. Since the operating conditions for each of the nozzles in this study were the same, if any of these effects were present they would be equally so for both the baseline nozzles and the mixer nozzles. This enables a useful evaluation of the axial vorticity mixing mechanism in the supersonic flow regime to be made.

A final noteworthy feature of the mixer nozzles is the high quality of internal and external flow that was present during these experiments. External-surface flow-visualization studies showed that there was no boundary-layer separation on any of the models. In addition, measured weightflow rates indicated that the mixer-nozzle flow coefficients were approximately the same as those for the baseline nozzles, within the uncertainty of the measurement. The measured value of the splayed-nozzle flow coefficient was approximately 0.96, while that for the rectangular nozzle was between 0.97 and 0.98. The estimated uncertainty in this measurement is  $\pm 0.01$ . These findings demonstrate that the mixer nozzles in general possess good aerodynamic characteristics, which is important if they are to be considered in exhaust-system applications.

### Conclusions

The overall issue addressed in this article was the enhancement of mixing rates in supersonic jet flows by the use of mixer nozzles. Specifically, high-temperature, supersonic jet mixing in the presence of an unconfined, subsonic coflowing stream was investigated. Enhanced supersonic jet mixing is important in a number of applications, including jet noise reduction and improved mixing within engine combustors. Recent investigations have shown that enhanced mixing between the primary and secondary streams in ejectors is of interest due to increased ejector performance benefits.

In the present study, mixer-nozzle models were tested in a high-temperature, supersonic primary flow environment in the presence of an unconfined subsonic wind-tunnel airstream. Jet mixing was characterized by mapping the total-temperature, total-pressure, static pressure, and velocity distributions at various points within the jet. Baseline models of conventional shape (circular and rectangular) were also evaluated so that mixer-nozzle effectiveness could be properly assessed. The baseline models were found to follow a predictable, conventional mixing process as observed by previous investigators.

The principal conclusions from this study are as follows. First, the splayed mixer-nozzle design was shown to provide significant improvements in jet mixing rate relative to the conventional baseline nozzles. A reduction in potential core length of approximately a factor of two relative to the baseline rectangular nozzle was achieved, with no penalty in the near-field downstream decay rate. The near-field decay rate was actually increased relative to the rectangular nozzle. This demonstrates the viability of the axial vortex mixing mechanism in

the high-temperature, supersonic flow environment. This experiment also provided a set of data for use in assessing CFD procedures for the calculation of complex, three-dimensional jet flowfields. Initial efforts in this area have already begun.<sup>35</sup>

In addition to these findings, the mixer nozzles were found to possess good internal and external aerodynamic characteristics. Flow-visualization studies revealed no external surface boundary-layer separation on any of the nozzles, and weight-flow measurements indicated that the splayed nozzle is internally aerodynamically similar to the baseline nozzles. This indicates that in addition to providing mixing benefits, the mixer nozzles are capable of functioning in jet applications where aerodynamic performance is important.

### Acknowledgments

The research described in this article was performed under funding provided by the United Technologies Research Center corporate-sponsored internal research program in gas dynamics, and by the Department of the Navy, Naval Air Systems Command, under Contract N00014-85-C-0506.

The authors wish to acknowledge specific contributions to this effort made by Walter M. Presz Jr. of Western New England College, by Stanley A. Skebe of United Technologies Research Center, and by James Lewis and Michael Willard of Pratt & Whitney, for their respective efforts relative to mixer-nozzle design, analysis of rectangular jet mixing, and supersonic nozzle scaling. Appreciation is also expressed to Karl Winckel (UTRC) and George Derderian (NAVAIR) for helpful discussions during the conduct of the research.

### References

- Tillman, T. G., Patrick, W. P., and Paterson, R. W., "Enhanced Mixing of Supersonic Jets," AIAA Paper 88-3002, July 1988.
- Lau, J. C., "Effects of Exit Mach Number and Temperature on Mean-Flow and Turbulence Characteristics in Round Jets," *Journal of Fluid Mechanics*, Vol. 105, April 1981, pp. 193-218.
- Lau, J. C., Morris, P. J., and Fisher, M. J., "Measurements in Subsonic and Supersonic Free Jets Using a Laser Velocimeter," *Journal of Fluid Mechanics*, Vol. 93, Pt. 1, July 1979, pp. 1-27.
- Sfeir, A. A., "The Velocity and Temperature Fields of Rectangular Jets," *Journal of Heat and Mass Transfer*, Vol. 19, Nov. 1976, pp. 1289-1297.
- Sforza, P. M., Steiger, M. H., and Trentacoste, N., "Studies on Three-Dimensional Viscous Jets," *AIAA Journal*, Vol. 4, No. 5, 1966, pp. 800-806.
- Sfeir, A. A., "Investigation of Three-Dimensional Turbulent Rectangular Jets," *AIAA Journal*, Vol. 17, No. 10, 1979, pp. 1055-1060.
- Sforza, P. M., and Stasi, W., "Heated Three-Dimensional Turbulent Jets," *Journal of Heat Transfer*, Vol. 101, No. 5, 1979, pp. 353-358.
- Krothapalli, A., Hsia, Y., Baganoff, D., and Karamcheti, K., "On the Structure of an Underexpanded Rectangular Jet," Joint Institute for Aeronautics and Acoustics, Stanford Univ., JIAA TR-47, Stanford, CA, July 1982.
- Paynter, G. C., Birch, S. C., Spalding, D. B., and Tatchell, D. G., "An Experimental and Numerical Study of the 3-D Mixing Flows of a Turbofan Engine Exhaust System," AIAA Paper 77-204, Jan. 1977.
- Bevilaqua, P. M., "Evaluation of Hypermixing for Thrust Augmenting Ejectors," *Journal of Aircraft*, Vol. 11, No. 6, 1974, pp. 348-354.
- Bevilaqua, P. M., "Analytic Description of Hypermixing and Test of an Improved Nozzle," *Journal of Aircraft*, Vol. 13, No. 1, 1976, pp. 43-48.
- DeJoode, A. D., and Patankar, S. V., "Prediction of Three-Dimensional Turbulent Mixing in an Ejector," *AIAA Journal*, Vol. 16, No. 2, 1978, pp. 145-150.
- Paterson, R. W., "Turbofan Mixer Nozzle Flowfield—A Benchmark Experimental Study," *Journal of Engineering for Gas Turbines and Power*, Vol. 106, July 1984, pp. 692-698.
- Presz, W. M., Jr., Gousy, R., and Morin, B. L., "Forced Mixer Lobes in Ejector Designs," AIAA Paper 86-1614, June 1986.
- Presz, W. M., Jr., Blinn, R. F., and Morin, B. L., "Short Effluent Ejector Systems," AIAA Paper 87-1837, June 1987.
- Werle, M. J., Paterson, R. W., and Presz, W. M., Jr., "Flow Structure in a Periodic Axial Vortex Array," AIAA Paper 87-0610, Jan. 1987.



<sup>17</sup>Skebe, S. A., Paterson, R. W., and Barber, T. J., "Experimental Investigation of Three-Dimensional Forced Mixer Lobe Flow Fields," AIAA Paper 88-3785, July 1988.

<sup>18</sup>Gutmark, E., and Schadow, K. C., "Azimuthal Instabilities and Mixing Characteristics of a Small Aspect Ratio Slot Jet," AIAA Paper 87-0486, Jan. 1987.

<sup>19</sup>Husain, H. S., and Hussain, A. K. M. F., "Excited Elliptic Jets," AIAA Paper 85-0544, March 1985.

<sup>20</sup>Glass, D. R., "Effects of Acoustic Feedback on the Spread and Decay of Supersonic Jets," *AIAA Journal*, Vol. 6, No. 10, 1968, pp. 1890-1897.

<sup>21</sup>Gutmark, E., Schadow, K. C., and Bicker, C. J., "Mode Switching in Supersonic Circular Jets," AIAA Paper 88-3610, July 1988.

<sup>22</sup>Ho, C. M., "Mixing Processes in Free Shear Layers," AIAA Paper 86-0234, Jan. 1986.

<sup>23</sup>Ho, C. M., and Zhang, Y. Q., "On the Manipulation of Spreading Rates of Forced Mixing Layers," Univ. of Southern California, N00014-77-C-0314, Los Angeles, CA, Sept. 1981.

<sup>24</sup>Metcalfe, R., Menon, S., and Hussain, A. K. M. F., "Physics of the Mixing Layer: Direct Numerical Simulations and Experiments," AIAA Paper 87-1249, June 1987.

<sup>25</sup>Paterson, R. W., Vogt, P. G., and Foley, W. M., "Design and Development of the United Aircraft Research Laboratories Acoustic Research Tunnel," AIAA Paper 72-1005, Sept. 1972.

<sup>26</sup>Moffat, R. J., *Temperature—Its Measurement and Control in Science and Industry*, Vol. 3, Reinhold, New York, 1962, pp. 553-571.

<sup>27</sup>Moffat, R. J., "Gas Temperature Measurement: Direct Design of

Radiation Shielding," Stanford Univ., 68-517, Stanford, CA, 1968.

<sup>28</sup>Patrick, W. P., "Flowfield Measurements in a Separated and Reattached Flat Plate Turbulent Boundary Layer," NASA CR-4052, 1987.

<sup>29</sup>Pinckney, Z. S., "A Short Static Pressure Probe Design for Supersonic Flow," NASA TN D-7978, 1975.

<sup>30</sup>Simonich, J. C., Amiet, R. K., and Schlinker, R. H., "Jet Shielding of Jet Noise," NASA CR-3966, 1986.

<sup>31</sup>Greitzer, E. M., Paterson, R. W., and Tan, C. S., "An Approximate Substitution Principle for Viscous Heat Conducting Flows," *Proceedings from the Royal Society of London, A*, 401, London, Sept. 1985, pp. 163-193.

<sup>32</sup>Putnam, L. E., and Mercer, C. E., "Pitot-Pressure Measurements in Flowfields Behind a Rectangular Nozzle with Exhaust Jet for Free-Stream Mach Numbers of 0.00, 0.60, and 1.20," NASA TM-88990, 1986.

<sup>33</sup>Skebe, S. A., "An Investigation of Warm Rectangular Jets," United Technologies Research Center, UTRC87-51, East Hartford, CT, 1987.

<sup>34</sup>Corrsin, S., and Kistler, A. L., "Free-Stream Boundaries of Turbulent Flows," NACA 1244, 1955.

<sup>35</sup>Anderson, O. L., and Barber, T. J., "Three-Dimensional Analysis of Complex Hot Exhaust Plumes," AIAA Paper 88-3705, July 1988.

<sup>36</sup>Schetz, J. A., *Injection and Mixing in Turbulent Flow*, Vol. 68, Progress in Astronautics and Aeronautics, AIAA, New York, 1980, pp. 19-83.

<sup>37</sup>Weinstein, A. S., Osterle, J. F., and Forstall, W., "Momentum Diffusion from a Slot Jet into a Moving Secondary," *Journal of Applied Mechanics*, Vol. 23, Sept. 1956, pp. 437-443.